



Title	Optimum Hot Electron Production with Low-Density Foams for Laser Fusion by Fast Ignition
Author(s)	Lei, A.L.; Tanaka, K.A.; Kodama, R. et al.
Citation	Physical Review Letters. 2006, 96(25), p. 255006-1-255006-4
Version Type	VoR
URL	https://hdl.handle.net/11094/3439
rights	Lei, A.L., Tanaka, K.A., Kodama, R., Kumar, G.R., Nagai, K., Norimatsu, T., Yabuuchi, T., Mima, K., Physical Review Letters, 96, 25, 255006, 2006-06-30. "Copyright 2006 by the American Physical Society."
Note	

The University of Osaka Institutional Knowledge Archive : OUKA

<https://ir.library.osaka-u.ac.jp/>

The University of Osaka

Optimum Hot Electron Production with Low-Density Foams for Laser Fusion by Fast Ignition

A. L. Lei,^{1,2,3,*} K. A. Tanaka,¹ R. Kodama,¹ G. R. Kumar,⁴ K. Nagai,¹ T. Norimatsu,¹ T. Yabuuchi,¹ and K. Mima¹

¹*Institute of Laser Engineering, Osaka University, 2-6 Yamada-oka, Suita, Osaka 565-0871, Japan*

²*Shanghai Institute of Optics and Fine Mechanics, P.O. Box 800-211, Shanghai 201800, China*

³*Research Center of Laser Fusion, CAEP, Mianyang 621900, China*

⁴*Tata Institute of Fundamental Research, Mumbai 400005, India*

(Received 8 February 2006; published 30 June 2006)

We propose a foam cone-in-shell target design aiming at optimum hot electron production for the fast ignition. A thin low-density foam is proposed to cover the inner tip of a gold cone inserted in a fuel shell. An intense laser is then focused on the foam to generate hot electrons for the fast ignition. Element experiments demonstrate increased laser energy coupling efficiency into hot electrons without increasing the electron temperature and beam divergence with foam coated targets in comparison with solid targets. This may enhance the laser energy deposition in the compressed fuel plasma.

DOI: [10.1103/PhysRevLett.96.255006](https://doi.org/10.1103/PhysRevLett.96.255006)

PACS numbers: 52.57.Kk, 52.38.Kd, 52.50.Jm

The dream of energy generation by laser fusion has been pursued since the invention of the laser with continuous innovation in laser and target design. The recent invention of chirped pulse amplification [1] has given birth to reasonably compact relativistic intensity laser systems and has opened many new frontiers such as fast ignition (FI) of laser fusion [2]. In the FI scheme, a fuel shell is imploded by high energy, nanosecond laser beams, as in conventional fusion experiments [3], forming a high-density core plasma. At its maximum compression an intense laser is focused on the fuel to create a hot spot for ignition. This hot spot is due to plasma heating caused by hot electrons generated in the intense laser plasma interactions. Integrated experiments with innovative gold cone-in-shell targets have demonstrated effective heating of the core plasma from the intense laser generated hot electrons [4]. Core plasma ion temperature increases to 0.8–1 keV and ~ 1000 times thermal neutron enhancement have been achieved by injecting a 0.5 PW laser into a dense fuel [5]. This is clear proof of the feasibility and promise of the FI scheme with a larger energy, petawatt laser.

The energy coupling from the intense laser into the core plasma is the key issue in FI. With the gold cone-in-shell target design, the intense laser is focused on the inner tip of the gold cone to generate hot electrons. The electrons then propagate into the core plasma and deposit their energy there for heating. Increasing the energy conversion efficiency from the laser into hot electrons will enhance the heating of the core plasma. The energy conversion efficiency from the laser into hot electrons with solid targets may be enhanced through increasing the laser intensity [6].

However, increasing the laser intensity will simultaneously increase the hot electron temperature with solid targets, resulting in the reduction of the hot electron energy deposition efficiency into the core plasma. Integrated experiments with gold cone-in-shell targets have showed that 30% of 0.1 PW laser energy can be coupled into the core plasma, while the coupling efficiency is reduced down to

$\sim 20\%$ for 0.5 PW laser [5]. The reduction of the laser energy coupling efficiency was attributed to the increase of the hot electron temperature when the laser power was increased. At ignition level, several 10 kJ laser energy is required and delivered within the disassembly time duration (several 10 ps) of fuel core plasma, resulting in the laser power equivalent to 1 PW or higher. At 1 PW, the laser energy coupling efficiency would be further reduced as the temperature of hot electrons becomes even higher.

Methods to increase the energy conversion efficiency from the laser into hot electrons without increasing the electron temperature are therefore of great importance for FI. We here propose to utilize metal or plastic foams for this purpose. Our proposed foam cone-in-shell target design for FI is based upon the gold cone-in-shell target design [4] and schematically shown in Fig. 1. The inner tip of a gold cone is covered with a thin low-density foam layer. The intense laser is focused on the foam instead of the solid-density cone tip to generate hot electrons for FI. Element experiments presented in this Letter demonstrate enhanced hot electron production without increasing the electron temperature and beam divergence from planar solid targets with thin low-density foam coating on the front surface. This indicates that our proposed foam cone-

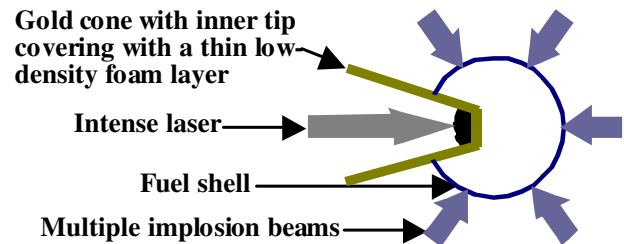


FIG. 1 (color online). Proposed foam cone-in-shell target design for the fast ignition, showing an intense laser irradiates the thin low-density foam layer which covers the inner tip of a gold cone inserted in a fuel shell.

in-shell target offers considerable improvements over the gold cone-in-shell target that has been successfully used for demonstrating the potential of FI.

To examine the feasibility of our proposed foam cone-in-shell target design for FI, we performed element experiments on both Gekko XII PW (GXII PW) laser and Gekko Module II (GMII) laser at the Institute of Laser Engineering, Osaka University. Both lasers had a prepulse with 10^{-8} contrast ratio by introducing optical parametric chirped pulse amplification system [7] and had pulse duration of about 0.6 ps. The *p*-polarized GXII PW laser and GMII laser irradiated the targets at 26° and 20° to the target normal, with energies on targets of about 100 and 10 J and the focus spot sizes of about 70 and 25 μm , respectively. The targets used were planar solid foils with front surface coating with low-density gold foams, resembling the gold cone inner tip covered with the low-density foam, as shown in Fig. 1. Planar solid targets without foam coating on the front surface were used as the references. Investigations were focused on the laser energy conversion efficiency into hot electrons, the hot electron temperature, and beam divergence.

Figure 2 shows the keV x-ray pinhole camera (XPHC) images taken from both the front and back of the targets irradiated by the GXII PW laser. The targets used were 20 μm thick molybdenum with front surface (i.e., laser interaction side) coating of either 2 μm solid gold or 2 μm gold foam. The density and porous cell size of the gold foam were 20% of the solid gold and about 0.3 μm [8]. The front XPHC monitored the laser interaction dynamics and had a 18 μm small pinhole with a 40 μm thick beryllium filter. The back XPHC monitored the heating of the rear surface of the target and had a 200 μm large pinhole with a 40 μm thick beryllium filter. Thus both XPHCs had the x-ray spectral sensitivity in the range over 1 keV, with an effective peak of the spectral response at about 5 keV. The front x-ray emission from the gold foam coated target is weaker than the solid gold coated target. However, the back x-ray emission from the gold foam coated target is much stronger than the solid gold coated target. The total count of the back x-ray emission from the gold foam coated target is about 3 times of the solid gold coated target. The back x-ray emission intensity reflects the deposited energy density located at the rear surface of the target and the heating of rear surface of the target. Higher x-ray emission count implies larger energy deposited. The deposited energy and heating are mainly from the hot electrons [9] generated at the front of the target during the laser interaction. These hot electrons propagate through the bulk target to heat the rear surface, resulting in the back x-ray emission. Note the x rays generated from the laser interactions at front surfaces cannot be responsible for the enhancement of the back x-ray emission from the gold foam coated target. The attenuation length of 5 keV x rays in molybdenum is

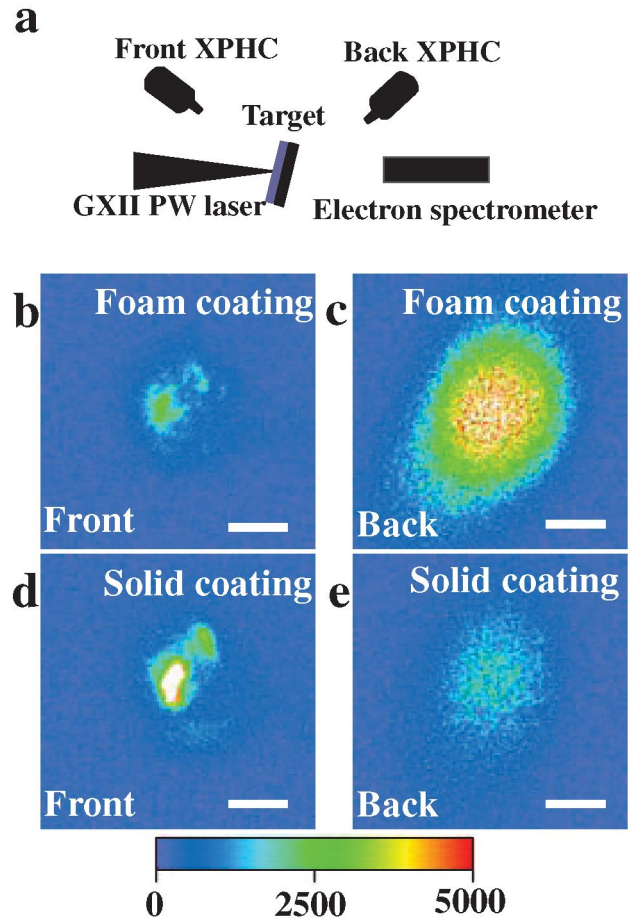


FIG. 2 (color). X-ray pinhole camera images taken from the front and back of the targets. (a) is the experimental setup. (b), (c) are the front and back images from the gold foam coated target; (d), (e) are the front and back images from the solid gold coated target, respectively. Both front images (b) and (d) show split spots due to poor laser focusing. The white scale bars correspond to 100 μm , given according to the distances from the target to the pinholes and the pinholes to the CCD cameras. The GXII PW laser energies were 113 J and 98 J for gold foam and solid gold coated targets, respectively.

only 1.8 μm and thus the target is too thick for keV x rays to transmit from the target front to the rear. Moreover, with gold foam coated target the x-ray emission from the target front is weaker, thus one would expect a weaker back x-ray emission, contrary to the experimental result, due to the x-ray transmission from the target front. We thus conclude that the gold foam coating on the front surface enables larger laser energy absorption and enhanced coupling into hot electrons. This in turn leads to larger amounts of surface heating and x-ray emission from the target rear.

Figure 3 shows the measured hot electron energy spectra with the same laser shots shown in Fig. 2. The hot electron spectra were measured with an electron spectrometer [10] placed behind the targets along the GXII PW laser axis, as

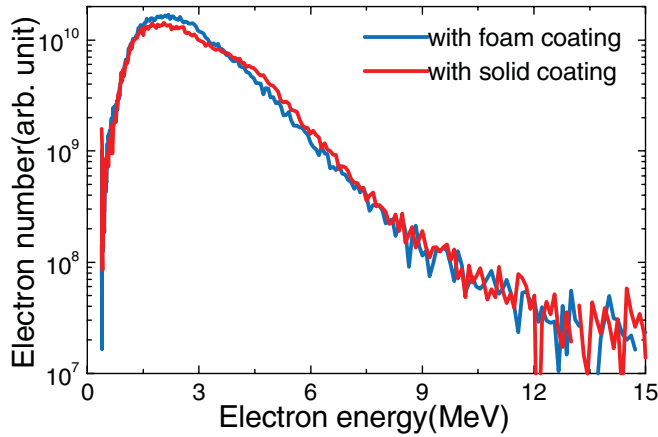


FIG. 3 (color). Measured hot electron energy spectra.

shown in Fig. 2(a). The hot electron spectra are very similar for solid gold coated and gold foam coated targets, showing a temperature ~ 1.5 MeV, a typical value for solid aluminum targets. We note that there is no comparable increase in the amount of the observed electron numbers with the gold foam coated target, unlike the back x-ray emissions. The crucial difference between the x-ray and electron measurements is the limitation on the electron current allowed in vacuum, behind the target. The electron spectrometer only detects the escaped electrons into vacuum and the amount of the electrons observed are heavily limited by the Alfvén limit and strong electrostatic potential formation by the hot electrons [11].

We attribute the enhanced hot electron production from the gold foam coated target (as evidenced by the x-ray emissions shown in Fig. 2) to the microstructure of the foam. Structuring the target surface reduces the laser reflectivity and significantly increases the laser absorption [12–15]. It has been shown that the microstructured targets, such as gratings and gold black [12], “velvet” coatings [13], porous and nanocylinder [14], and metal nanoparticle coatings [15], are more efficient at absorbing the intense laser energy than the polished solid targets. As a result, significant enhancements have been demonstrated in emissions of soft x rays [12–14], and hard x rays [15], which is a signature of hot electrons created in the laser interactions. The use of a low-density foam covering the gold cone tip, as shown in Fig. 1, can be thus expected to facilitate highly efficient conversion of the laser into hot electrons simultaneously without increasing the electron temperature for FI.

We have also examined the hot electron energy spectrum with 1700 μm thick 160 mg/cc deuterated carbon (CD) foam target with the GXII PW laser. The measured electron temperature was 1.1 MeV, lower than that for a solid target. This softening of hot electron temperature was also observed with the CD foam target with the GMII laser [16]. The reduction of the hot electron temperature is due to either low temperature of the hot electrons at the source or

the low-density effect on the hot electron transport inside the CD foam. The electron transport can be severely suppressed by the induced strong electric field inside the low-density insulator foam [17]. However, the hot electron energy spectra have been experimentally shown not to be influenced by the electron transport inside the foams varying densities and thicknesses [18]. This suggests that the reduction of the electron temperature with the CD foam target in our experiment is due to the low temperature at the source. The hot electron temperature can possibly be reduced (controlled) to an optimum value by adjusting the thickness of the foam.

The use of the low-density foam enhances the production of hot electrons without increasing their temperature, which is good for the heating of the core plasma. We have to also examine the foam effect on the hot electron beam divergence. A collimated electron beam minimizes the heating volume of the core plasma and thus the laser energy required for ignition. Particular concern on the foam effect is the inhibition of hot electron transport inside the foam due to induced strong electric field. The magnitude of the field depends on the conductivity of the target material. To mitigate the inhibition of the hot electron transport for our purpose here, we consider utilizing high-Z foams, which might have higher conductivity than low-Z foams. We also consider minimizing the foam thickness so as to reduce the length of hot electron transport inside the foam while keeping the foam sufficiently thick to efficiently absorb the laser energy and enhance the hot electron production.

We therefore utilize the high-Z gold foam with thickness of 10 μm . To examine the gold foam effect on the hot electron beam divergence, we have directly measured the angular distribution of hot electrons emitted from the target rear surface with an imaging plate (IP) (Fuji BAS-SR2025), as shown in Fig. 4(a). A stack consisting of an aluminum foil and a plastic plate was placed in front of the IP to prevent any optical light and ions from striking the IP. This leads to the detected electrons in the energy range higher than 450 keV. The target used was 10 μm thick solid gold foil with 10 μm thick gold foam coating on the front surface. The thickness of the solid gold is close to the tip thickness of the gold cone [4]. Solid gold foil target with thickness of 12 μm was used for comparison. The areal density is kept the same for these two targets. Since the rear surface of the target was same, the hot electron divergence difference thus reflects the difference in hot electron generation and transport with and without gold foam coating. Figure 4 shows the measured hot electron emission angular distributions. The electron emissions from both targets, as shown in Fig. 4(b)–4(d), peaked at the target rear normal, indicating the electron production is mainly due to the vacuum heating absorption. There was no filament or split spot observed in the hot electron emission from the gold foam coated target. Such filamentary structures appear in

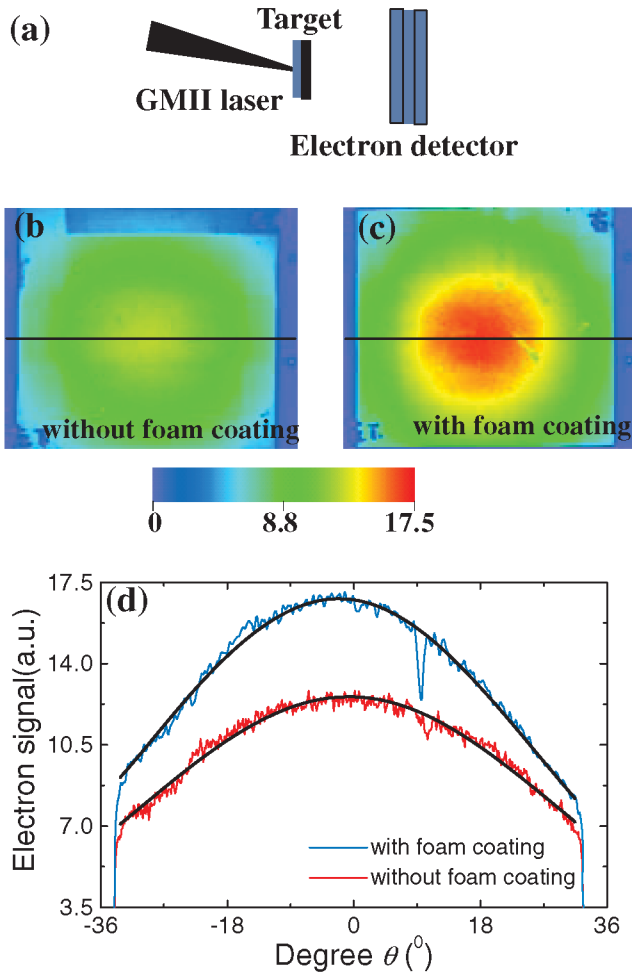


FIG. 4 (color). Measured hot electron angular distributions. (a) is the experimental setup. (b), (c) are the hot-electron images without or with the gold foam coated targets, respectively. (d) shows the hot-electron signal intensity profiles from the horizontal black lines in (b) and (c). The degree 0° corresponds to the normal direction of the target rear. The fitted curves in black with a Gaussian distribution are also shown.

the case of thick insulator foams [16,18]. The hot electron beam patterns shown in Fig. 4(b) and 4(c) for both the gold foam coated target and solid gold target are quite smooth and spatially Gaussian. The electron signal profiles shown in Fig. 4(d) can be well fitted with a Gaussian distribution $S_{\text{signal}} \propto e^{-(\theta-\theta_0)^2/(2\sigma^2)}$ with $\theta_0 \approx 0$ and $\sigma = 30.4$ and 28 for the solid and foam coated targets, respectively. This gives the full width at half maximum of the hot electron beam divergence to be 72° and 66° for the solid and foam coated targets, respectively. The electron beam divergence

is quite similar with and without gold foam coating, indicating that the electron propagation into the target (and hence the heated volume) is similar in both cases.

In summary, we propose a novel foam cone-in-shell target design for the FI of laser fusion. We report element experiment results which show that the use of thin high-Z low-density foam enhances laser energy conversion into hot electrons without increasing the electron temperature and beam divergence. This offers a strong indication that the proposed target design potentially enables enhanced heating of the core plasma and hence has advantages over the gold cone-in-shell target successfully used for demonstrating FI. Our results also show a possibility for optimizing the thickness and density of the foam so as to reduce or optimize the hot electron temperature for FI. Such an optimization and better understanding of the intense laser-foam interactions, however, need particle-in-cell (PIC) simulations [16,19] or Vlasov simulations [20]. The complex 3D structure of the foam needs to be considered in the simulation.

Part of this research is supported by the JSPS Japan-China core university program. A.L.L. acknowledges JSPS for support.

*Electronic address: lal@ile.osaka-u.ac.jp

- [1] D. Strickland and G. Mourou, *Opt. Commun.* **56**, 219 (1985).
- [2] M. Tabak *et al.*, *Phys. Plasmas* **1**, 1626 (1994).
- [3] J. Lindl, *Phys. Plasmas* **2**, 3933 (1995).
- [4] R. Kodama *et al.*, *Nature (London)* **412**, 798 (2001).
- [5] R. Kodama *et al.*, *Nature (London)* **418**, 933 (2002).
- [6] M.H. Key *et al.*, *Phys. Plasmas* **5**, 1966 (1998).
- [7] Y. Kitagawa *et al.*, *IEEE J. Quantum Electron.* **40**, 281 (2004).
- [8] K. Nagai *et al.*, *Fusion Sci. Technol.* **49**, 686 (2006).
- [9] E. Martinolli *et al.*, *Phys. Rev. E* **70**, 055402(R) (2004).
- [10] K.A. Tanaka *et al.*, *Rev. Sci. Instrum.* **76**, 013507 (2005).
- [11] T. Yabuuchi *et al.* (to be published).
- [12] M.M. Murnane *et al.*, *Appl. Phys. Lett.* **62**, 1068 (1993).
- [13] G. Kulscár *et al.*, *Phys. Rev. Lett.* **84**, 5149 (2000).
- [14] T. Nishikawa *et al.*, *Appl. Phys. Lett.* **70**, 1653 (1997); T. Nishikawa *et al.*, *Appl. Phys. Lett.* **75**, 4079 (1999).
- [15] P.P. Rajeev *et al.*, *Phys. Rev. Lett.* **90**, 115002 (2003).
- [16] Y.T. Li *et al.*, *Phys. Rev. E* **72**, 066404 (2005).
- [17] D. Batani *et al.*, *Phys. Rev. E* **65**, 066409 (2002).
- [18] R. Jung *et al.*, *Phys. Rev. Lett.* **94**, 195001 (2005).
- [19] S. Okihara *et al.*, *Phys. Rev. E* **69**, 026401 (2004).
- [20] H. Ruhl *et al.*, *Phys. Rev. Lett.* **82**, 2095 (1999).